



Article

Plasma Electrochemical Synthesis of Graphene-Phosphorene Composite and Its Catalytic Activity towards Hydrogen Evolution Reaction

Valeriy K. Kochergin, Natal'ya S. Komarova, Alexander S. Kotkin, Roman A. Manzhos ^{*}, Vladimir P. Vasiliev ^{*} and Alexander G. Krivenko

Federal Research Center of Problems of Chemical Physics and Medicinal Chemistry of Russian Academy of Sciences, Chernogolovka 142432, Russia

^{*} Correspondence: rmanzhos@yandex.ru (R.A.M.); vpvasiliev@mail.ru (V.P.V.)

Abstract: For the first time, graphene-phosphorene structures were synthesized using the plasma-assisted electrochemical method. The catalytic activity of the composite obtained in the electrolytic plasma mode and its mixtures with few-layer graphene structures toward the hydrogen evolution reaction was studied. A substantial increase in the catalytic activity of the phosphorene structures towards the hydrogen evolution reaction was realized by mixing them with few-layer graphene structures. The catalyst demonstrates excellent activity towards the hydrogen evolution reaction in alkaline media with a low overpotential of 940 mV at a current density of 10 mA·cm⁻² and a small Tafel slope of 130 mV dec⁻¹.

Keywords: phosphorene; few-layer graphene structures; electrolytic plasma; electrochemical exfoliation of graphite; hydrogen evolution reaction



Citation: Kochergin, V.K.; Komarova, N.S.; Kotkin, A.S.; Manzhos, R.A.; Vasiliev, V.P.; Krivenko, A.G. Plasma Electrochemical Synthesis of Graphene-Phosphorene Composite and Its Catalytic Activity towards Hydrogen Evolution Reaction. *C* **2022**, *8*, 79. <https://doi.org/10.3390/c8040079>

Academic Editor: Manuel Fernando Ribeiro Pereira

Received: 10 November 2022

Accepted: 10 December 2022

Published: 14 December 2022

Publisher's Note: MDPI stays neutral with regard to jurisdictional claims in published maps and institutional affiliations.



Copyright: © 2022 by the authors. Licensee MDPI, Basel, Switzerland. This article is an open access article distributed under the terms and conditions of the Creative Commons Attribution (CC BY) license (<https://creativecommons.org/licenses/by/4.0/>).

1. Introduction

Compared to other allotropes, layered black phosphorus (BP) is the most thermodynamically stable and has a relatively high conductivity; see, for example, review [1]. Moreover, black phosphorus is quite easily split into monolayer “corrugated” sheets, so-called phosphorene, consisting of two-layer six-membered rings, which, due to sp³ hybridization, resemble honeycomb graphene-like structures in a vertical projection [2]. A unique feature of phosphorene is the presence of a lone electron pair which can serve as an active center for chemical and electrochemical reactions.

It should be mentioned that, in the view of the “green” energy concept, hydrogen is of great interest as the cleanest fuel, which in the future could replace fossil fuels. Hydrogen is also used as a raw material in various chemical syntheses, for example, the synthesis of ammonia, for the purification of metals as well as in semiconductor manufacturing [3–5]. Of note, in the latter case, high purity hydrogen is required, which can only be produced using water electrolysis. Of particular importance, the hydrogen evolution reaction (HER), sustainable and facile, requires economical and efficient electrocatalysts to improve energy efficiency [6–8]. Despite the fact that Pt-based catalysts are widely used for HER due to the minimum binding energy of Pt with hydrogen, their high cost and scarce resources limit their widespread application in water electrolysis. Hence, the development of highly efficient and low-cost noble metal-free hydrogen evolution reaction catalysts is an important research direction in this field. According to modern notions [9,10], phosphorene structures can be utilized as a promising component of the catalysts of the hydrogen evolution reaction and the electrochemistry of organic compounds, and their electrocatalytic characteristics can be greatly enhanced by doping or functionalization.

According to the data in the literature, three methods of phosphorene production from bulk BP are the most widely used, namely, ultrasonic liquid exfoliation [1], electrochemical

exfoliation [11,12], and grinding in a ball mill [13]. Electrocatalytic studies of electrodes with a predominantly basal and edge orientation of black phosphorus demonstrated a significantly higher catalytic activity of the edges. This can be explained by theoretical calculations which predict the semiconductor nature of the basal plane and the metallic behavior of the BP edges [14]. To increase catalytic activity, in addition to the orientation of phosphorene layers on the electrode surface, a number of other methods have been proposed: the doping of black phosphorus with nitrogen during grinding in a ball mill with the addition of urea [15] and the combination of phosphorene with other active materials [16,17], such as MoS₂ and Ni₂P. In these works, a significant increase in the catalytic activity towards the hydrogen evolution reaction after the modification of phosphorene was explained not by an increase in the active center number but by an increase in the density of the charge carriers by three orders of magnitude. In [18], the traditional method of increasing the catalytic activity towards the HER was realized by embellishing phosphorene with nanoparticles of noble metals, such as Pt, Ag, and Au; as a result, a higher activity of obtained catalysts was demonstrated compared to nanoparticles of these metals on a carbon substrate.

In the present work, the plasma-assisted electrochemical synthesis of a composite of graphene-phosphorene structures (GPS) is proposed and their catalytic activity toward the hydrogen evolution reaction is studied.

2. Experimental Procedure

Black phosphorus was obtained from red phosphorus by the solvothermal method [19,20]. Thus, 1–2 g of red phosphorus (reagent grade, Sigma Aldrich, St. Louis, MO, USA) was carefully ground underwater in a jade mortar, and the resulting aqueous suspension was placed in a 30 mL autoclave and kept in a muffle furnace at 190 °C for 24 h to purify phosphorus from its oxides. After cooling, the red phosphorus powder was washed thoroughly with water and then with alcohol and dried in a vacuum oven for 12 h at 60 °C. The resulting powder was dispersed in ethylenediamine (reagent grade, Sigma Aldrich, St. Louis, MO, USA). The preliminary suspension was purged with argon and placed in an autoclave for 12 h at 190 °C. After cooling, the resulting product was washed thoroughly with water and then with alcohol and dried in a vacuum oven for 12 h at 60 °C.

Graphene-phosphorene structures were synthesized in a one-stage process which was carried out using a homemade setup. The setup fed graphite electrodes immersed in an electrolyte solution with pulses of different polarity voltage U with an amplitude up to 300 V. Pulse duration was 10 ms and the rise time was ca. 0.5 μ s. The electrolytic plasma mode was realized due to a significant difference in the size of the graphite electrodes [21]. Nuclear graphite GR-280 was utilized. The black phosphorous exfoliation induced by electrolytic plasma was carried out in a Teflon reactor, which was a cylinder with holes in the side wall for the electrolyte; a schematic diagram of the reactor and its configuration in the cell is depicted in Figure 1. A total of 50 mg of BP powder was placed in the reactor and closed with a graphite rod tightly attached to the inner walls of the cylinder with a small taper at the tip. As a result, when the reactor was placed in a cell for exfoliation, the graphite rod was in the solution within ca. 0.5 cm line. The process was carried out in a 1 M Na₂SO₄ solution in the electrolytic plasma mode ($U = 300$ V). Sodium sulfate was of reagent grade purity from ChimMed (Moscow, Russia). After several stages of decantation and centrifugation, the resulting aqueous dispersion was transferred into a stable suspension of the nanocomposite in water with a concentration of ca 2 mg·mL⁻¹.

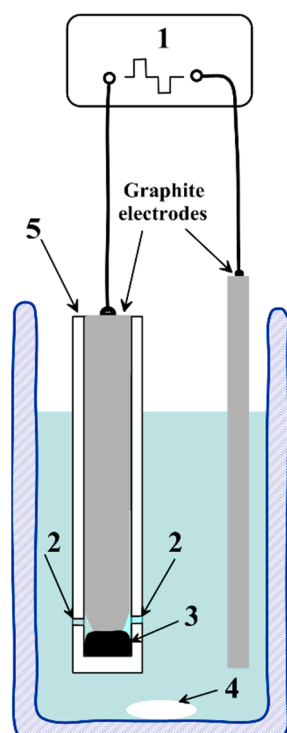


Figure 1. Schematic diagram of the reactor and cell configuration for the high-voltage pulse exfoliation of black phosphorus and graphite: 1—the source of high-voltage impulses, 2—holes for electrolyte, 3—black phosphorus, 4—magnetic stirrer, and 5—Teflon reactor.

Samples for scanning electron microscopy (SEM) and X-ray photoelectron spectroscopy (XPS) were prepared as follows. The ultrasonicated suspension of the GPS composite was drop-cast onto the surface of a silicon substrate and air-dried at ambient temperature. The SEM images were obtained using a scanning electron microscope, Zeiss SUPRA 25 (Carl Zeiss, Jena, Germany), equipped with an energy dispersive X-ray spectroscopy (EDX) analysis EDS detector. XPS spectra were acquired on a Specs PHOIBOS 150 MCD electron spectrometer (Specs, Berlin, Germany) equipped with an Mg cathode ($h\nu = 1253.6$ eV). During spectra measurements, the vacuum in the spectrometer chamber was less than 4×10^{-8} Pa. The constant transmission energy mode was used to record spectra; 40 eV for survey spectra and 10 eV for individual lines. The survey spectrum was taken in 1.00 eV increments, and the individual line spectra were gathered in 0.03 eV increments. The Shirley method [22] was used to subtract the background, and the CasaXPS software (version 2.3.19, Casa Software Ltd., Teignmouth, UK) was used for spectra deconvolution. The atomic content was quantified with respect to the sensitivity factors from the CasaXPS elemental library. The analyzed area was 300–700 mm² with an information depth of 1–2 nm.

The hydrogen evolution reaction was studied by linear-sweep voltammetry (LSV) carried out in a three-electrode cell with the usage of a VED-06 rotating disk electrode setup (Volta Ltd., Saint-Petersburg, Russia) and an IPC Pro-L potentiostat (A.N. Frumkin Institute of Physical Chemistry and Electrochemistry, RAS, Moscow, Russia). The working electrode was a glassy carbon (GC) disc (\varnothing 3 mm) pressed in Teflon and the counter electrode was platinum foil. The reference electrode was Ag/AgCl (sat. KCl). A total of 7 μ L of the aqueous suspension of composite (ca. 2 mg·mL⁻¹) with ca. 0.1 wt.% of Nafion polymer was drop-cast onto the glassy carbon electrode and then dried in the ambient environment. Therefore, the catalyst loading was ca. 200 μ g·cm⁻². The LSV measurements were carried out in an Ar-saturated 0.1 M KOH solution at a potential scan rate $\nu = 10$ mV·s⁻¹ and electrode rotation rate of 2000 rpm.

3. Results and Discussion

The scanning electron microscopy images of the synthesized graphene-phosphorene nanocomposite are presented in Figure 2. As can be seen, the composite consists of partially agglomerated few-layer graphene structures (FLGS) whose surface is fully covered with phosphorene particles. FLGS are graphene-like particles with rough edges with characteristic lateral sizes of 0.05–1 μm and a thickness of 2–5 nm; the phosphorene particles are grains 100–200 nm in size. According to the EDX data, during 1 h of synthesis, composites containing few-layer graphene structures not exceeding 25 wt.% were obtained.

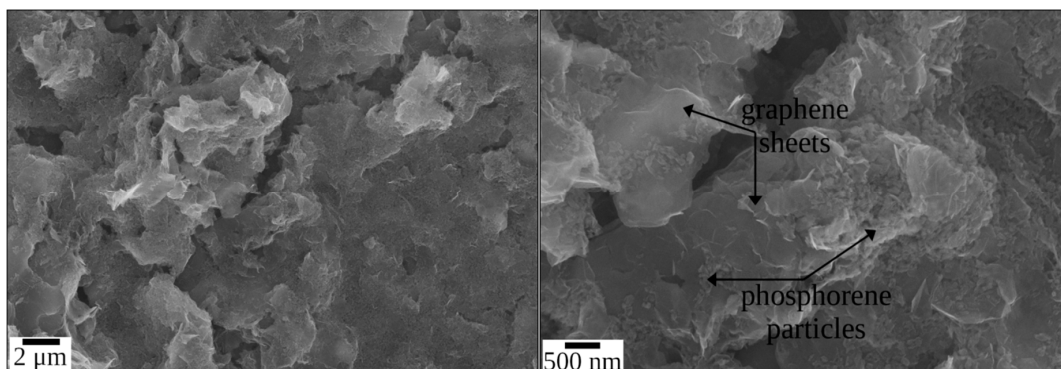


Figure 2. SEM images of the graphene-phosphorene composite at different magnifications.

The results of the XPS elemental analysis of the surface of the GPS composite are presented in Table 1. According to [23,24], sulfur can be attributed to the C–SO₂ and C–SO₃ groups. Oxygen-containing groups can be identified by means of the analysis of C 1s high-resolution XPS spectrum. The Doniach/Sunjic hybrid function [25] was used to consider the asymmetry observed for the main C 1s peak. Figure 3 shows the C 1s spectrum of the graphene-phosphorene composite sample and its deconvolution into individual peaks. The peak assignment was performed mainly on basis of [26–30] and the obtained surface concentrations of oxygen-containing groups are presented in Table 2. As is seen, the oxygen-containing groups on the surface of the FLGS component of the GPS composite are mainly C=O and hydroxyl/epoxy ones. The concentrations of these groups are slightly less than those of the FLGS obtained in the electrolytic plasma mode [23]. P 2p high-resolution spectrum of graphene-phosphorene composite (Figure 4) can be represented by two peaks at 129.5 and 128.6 eV which correspond to the 2p_{1/2} and 2p_{3/2} states of elemental phosphorus, respectively [20].

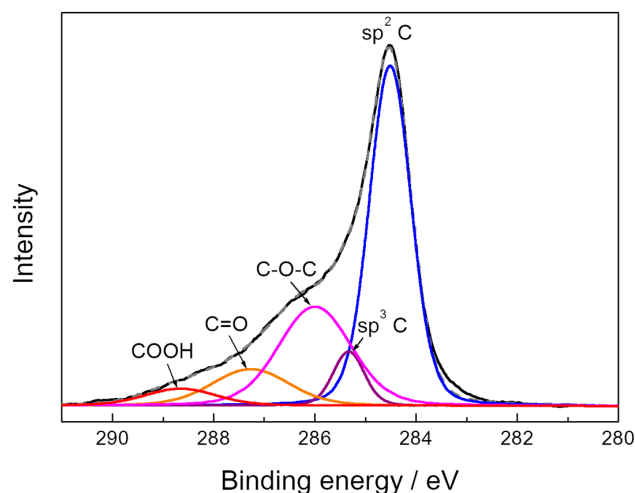


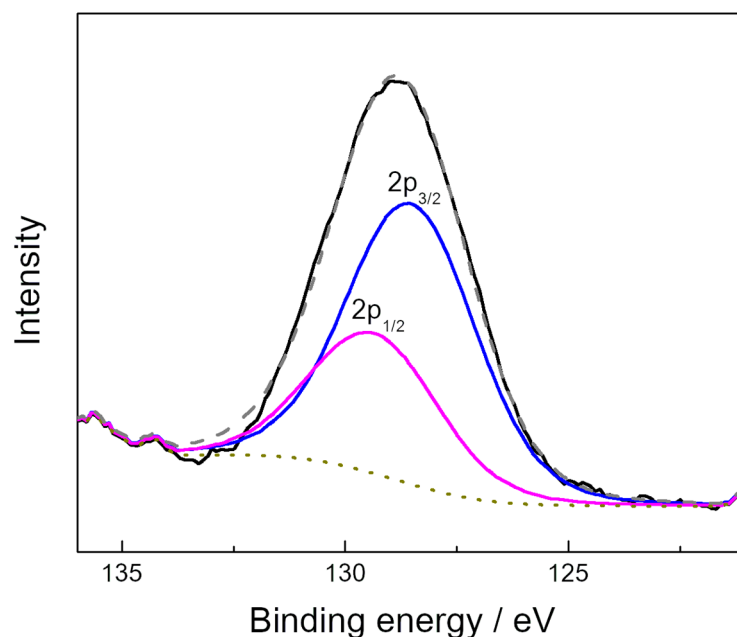
Figure 3. C 1s high-resolution spectrum of the graphene-phosphorene composite.

Table 1. Elemental composition of the GPS surface.

C, at.%	O, at.%	P, at.%	S, at.%
68.6	19.4	10.9	1.1

Table 2. Content of the oxygen-containing groups on the GPS surface.

C–O–C, at.%	C=O, at.%	COOH, at.%
12.5	4.9	1.0

**Figure 4.** P 2p high-resolution spectrum of the graphene-phosphorene composite.

To study the catalytic activity towards the hydrogen evolution reaction, mixtures of the obtained composite with few-layer graphene structures synthesized in the electrolytic plasma mode [23] were prepared. Figure 5 shows LSVs for the GC electrodes covered with FLGS, a composite of graphene-phosphorene structures, and the GPS/FLGS mixture (1:1 weight ratio) in an Ar-saturated solution of 0.1 M KOH. As can be seen, the HER overpotential decreases in the series FLGS, GPS, and GPS/FLGS (1:1). Obviously, the graphene-phosphorene composite demonstrates higher currents of hydrogen evolution due to the phosphorene which acts as an HER catalyst. Thus, the highest catalytic activity towards the hydrogen evolution reaction, exceeding that for each separate component, was demonstrated by the composition containing equal mass amounts of the GPS composite and FLGS. The overpotential values at $10 \text{ mA}\cdot\text{cm}^{-2}$ for FLGS, GPS, and GPS/FLGS (1:1) are 1150, 1080, and 940 mV, respectively. Tafel plots presented in the inset in Figure 5 show slopes at 250, 200, and $130 \text{ mV}\cdot\text{dec}^{-1}$ for FLGS, GPS, and GPS/FLGS (1:1), respectively. The smallest value of the Tafel slope for the GPS/FLGS composite argues for the best catalytic performance in the HER of this sample. This effect can be explained by the increase in conductivity [17,31,32] of the GPS/FLGS mixture in comparison with the initial graphene-phosphorene composite. Namely, few-layer graphene structures act as conductive substrates, and phosphorene particles are more evenly distributed in the catalyst layer. Therefore, more active centers become accessible to the electrolyte, which leads to an increase in catalytic activity towards the HER. This interesting synergistic effect should be studied in more detail in the future.

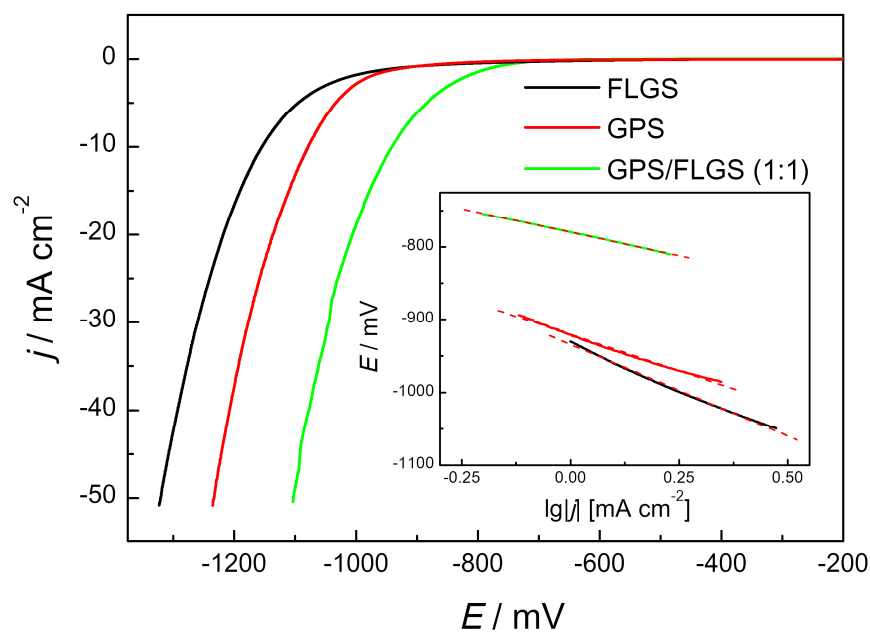


Figure 5. The hydrogen evolution reaction with different catalysts in an Ar-saturated 0.1 M KOH solution, $v = 10 \text{ mV} \cdot \text{s}^{-1}$, and an electrode rotation rate of 2000 rpm. The inset shows the corresponding Tafel plots.

4. Conclusions

The plasma-assisted electrochemical synthesis of graphene-phosphorene structures has been carried out for the first time. In this paper, the catalytic activity towards the hydrogen evolution of the GPS composite and its mixtures with few-layer graphene structures was studied. A substantial increase in the catalytic activity of phosphorene structures towards the hydrogen evolution reaction was realized by mixing them with few-layer graphene structures, due to the increase in the electrical conductivity of the resulting composite. The present work demonstrates that combining graphene-phosphorene and few-layer graphene structures is an efficient approach to designing an HER electrocatalyst.

Author Contributions: Conceptualization, A.G.K.; Data curation, V.K.K., V.P.V. and R.A.M.; Formal analysis, N.S.K. and A.S.K.; Investigation, N.S.K., V.K.K. and R.A.M.; Methodology, R.A.M. and A.G.K.; Project administration, R.A.M. and A.G.K.; Resources, A.S.K.; Supervision, A.G.K.; Validation, V.K.K. and R.A.M.; Visualization, N.S.K.; Writing—original draft, V.K.K., R.A.M. and A.G.K.; Writing—review and editing, V.K.K., V.P.V. and A.G.K. All authors have read and agreed to the published version of the manuscript.

Funding: Russian Science Foundation (grant no. 22-23-00774).

Institutional Review Board Statement: Not applicable.

Informed Consent Statement: Not applicable.

Data Availability Statement: All data available are provided in the article.

Acknowledgments: This study is supported by the Russian Science Foundation (grant no. 22-23-00774) and performed with the equipment of the Multi-User Analytical Center of FRC PCP MC RAS.

Conflicts of Interest: The authors declare no conflict of interest.

References

1. Li, B.; Lai, C.; Zeng, G.; Huang, D.; Qin, L.; Zhang, M.; Fu, Y. Black Phosphorus, a Rising Star 2D Nanomaterial in the Post-Graphene Era: Synthesis, Properties, Modifications, and Photocatalysis Applications. *Small* **2019**, *15*, 1804565. [[CrossRef](#)] [[PubMed](#)]
2. Nilges, T.; Kersting, M.; Pfeifer, T. A Fast Low-Pressure Transport Route to Large Black Phosphorus Single Crystals. *J. Solid State Chem.* **2008**, *181*, 1707–1711. [[CrossRef](#)]
3. Bockris, J.O.M. The Hydrogen Economy: Its History. *Int. J. Hydrogen Energy* **2013**, *38*, 2579–2588. [[CrossRef](#)]
4. Pudukudy, M.; Yaakob, Z.; Mohammad, M.; Narayanan, B.; Sopian, K. Renewable Hydrogen Economy in Asia—Opportunities and Challenges: An Overview. *Renew. Sustain. Energy Rev.* **2014**, *30*, 743–757. [[CrossRef](#)]
5. Miyazaki, J.; Kajiyama, T.; Matsumoto, K.; Fujiwarat, H.; Yatabe, M. Ultra High Purity Hydrogen Gas Supply System with Liquid Hydrogen. *Int. J. Hydrogen Energy* **1996**, *21*, 335–341. [[CrossRef](#)]
6. Zhao, G.; Rui, K.; Dou, S.X.; Sun, W. Heterostructures for Electrochemical Hydrogen Evolution Reaction: A Review. *Adv. Funct. Mater.* **2018**, *28*, 1803291. [[CrossRef](#)]
7. Chen, Y.; Wang, X.; Lao, M.; Rui, K.; Zheng, X.; Yu, H.; Ma, J.; Dou, S.X.; Sun, W. Electrocatalytically Inactive SnS₂ Promotes Water Adsorption/Dissociation on Molybdenum Dichalcogenides for Accelerated Alkaline Hydrogen Evolution. *Nano Energy* **2019**, *64*, 103918. [[CrossRef](#)]
8. Lao, M.; Rui, K.; Zhao, G.; Cui, P.; Zheng, X.; Dou, S.X.; Sun, W. Platinum/Nickel Bicarbonate Heterostructures towards Accelerated Hydrogen Evolution under Alkaline Conditions. *Angew. Chem. Int. Ed.* **2019**, *58*, 5432–5437. [[CrossRef](#)]
9. He, L.; Lian, P.; Zhu, Y.; Lu, Q.; Wang, C.; Mei, Y. Review on Applications of Black Phosphorus in Catalysis. *J. Nanosci. Nanotechnol.* **2019**, *19*, 5361–5374. [[CrossRef](#)]
10. Dinh, K.N.; Zhang, Y.; Zhu, J.; Sun, W. Phosphorene-Based Electrocatalysts. *Chem. Eur. J.* **2020**, *26*, 6437–6446. [[CrossRef](#)]
11. Ambrosi, A.; Sofer, Z.; Pumera, M. Electrochemical Exfoliation of Layered Black Phosphorus into Phosphorene. *Angew. Chem. Int. Ed.* **2017**, *56*, 10443–10445. [[CrossRef](#)] [[PubMed](#)]
12. Xiao, H.; Zhao, M.; Zhang, J.; Ma, X.; Zhang, J.; Hu, T.; Wu, H. Electrochemical Cathode Exfoliation of Bulky Black Phosphorus into Few-Layer Phosphorene Nanosheets. *Electrochem. Commun.* **2018**, *89*, 10–13. [[CrossRef](#)]
13. Liu, W.; Zhu, Y.; Xu, X.; Wang, S.; Zhang, X. Preparation of Few-Layer Black Phosphorus by Wet Ball Milling Exfoliation. *J. Mater. Sci. Mater. Electron.* **2020**, *31*, 9543–9549. [[CrossRef](#)]
14. Sofer, Z.; Sedmidubský, D.; Huber, Š.; Luxa, J.; Bouša, D.; Boothroyd, C.; Pumera, M. Layered Black Phosphorus: Strongly Anisotropic Magnetic, Electronic, and Electron-Transfer Properties. *Angew. Chem. Int. Ed.* **2016**, *55*, 3382–3386. [[CrossRef](#)]
15. Shao, L.; Sun, H.; Miao, L.; Chen, X.; Han, M.; Sun, J.; Chen, J. Facile Preparation of NH₂-Functionalized Black Phosphorene for the Electrocatalytic Hydrogen Evolution Reaction. *J. Mater. Chem. A* **2018**, *6*, 2494–2499. [[CrossRef](#)]
16. Batmunkh, M.; Bat-Erdene, M.; Shapter, J.G. Phosphorene and Phosphorene-Based Materials—Prospects for Future Applications. *Adv. Mater.* **2016**, *28*, 8586–8617. [[CrossRef](#)]
17. Luo, Z.-Z.; Zhang, Y.; Zhang, C.; Tan, H.T.; Li, Z.; Abutaha, A.; Yan, Q. Multifunctional 0D-2D Ni₂P Nanocrystals-Black Phosphorus Heterostructure. *Adv. Energy Mater.* **2016**, *7*, 1601285. [[CrossRef](#)]
18. Peng, Y.; Lu, B.; Wang, N.; Lu, J.E.; Li, C.; Ping, Y.; Chen, S. Oxygen Reduction Reaction Catalyzed by Black Phosphorus-Supported Metal Nanoparticles: Impacts of Interfacial Charge Transfer. *ACS Appl. Mater. Interfaces* **2019**, *11*, 24707–24714. [[CrossRef](#)]
19. Ozawa, A.; Yamamoto, M.; Tanabe, T.; Hosokawa, S.; Yoshida, T. Black Phosphorus Synthesized by Solvothermal Reaction from Red Phosphorus and Its Catalytic Activity for Water Splitting. *J. Mater. Chem. A* **2020**, *8*, 7368–7376. [[CrossRef](#)]
20. Wang, Y.; He, M.; Ma, S.; Yang, C.; Yu, M.; Yin, G.; Zuo, P. Low-Temperature Solution Synthesis of Black Phosphorus from Red Phosphorus: Crystallization Mechanism and Lithium Ion Battery Applications. *J. Phys. Chem. Lett.* **2020**, *11*, 2708–2716. [[CrossRef](#)]
21. Krivenko, A.G.; Manzhos, R.A.; Kotkin, A.S.; Kochergin, V.K.; Piven, N.P.; Manzhos, A.P. Production of Few-Layer Graphene Structures in Different Modes of Electrochemical Exfoliation of Graphite by Voltage Pulses. *Instrum. Sci. Technol.* **2019**, *47*, 535–544. [[CrossRef](#)]
22. Shirley, D.A. Hyperfine Interactions and ESCA Data. *Phys. Scr.* **1975**, *11*, 117–120. [[CrossRef](#)]
23. Vasiliev, V.P.; Kotkin, A.S.; Kochergin, V.K.; Manzhos, R.A.; Krivenko, A.G. Oxygen Reduction Reaction at Few-Layer Graphene Structures Obtained via Plasma-Assisted Electrochemical Exfoliation of Graphite. *J. Electroanal. Chem.* **2019**, *851*, 113440. [[CrossRef](#)]
24. Vasiliev, V.P.; Manzhos, R.A.; Krivenko, A.G. Electrical Conductivity of Films Formed by Few-Layer Graphene Structures Obtained by Plasma-Assisted Electrochemical Exfoliation of Graphite. *Int. J. Electrochem.* **2019**, *2019*, 6478708. [[CrossRef](#)]
25. Doniach, S.; Sunjic, M. Many-Electron Singularity in X-ray Photoemission and X-ray Line Spectra from Metals. *J. Phys. C Solid State Phys.* **1970**, *3*, 285–291. [[CrossRef](#)]
26. Yamada, Y.; Yasuda, H.; Murota, K.; Nakamura, M.; Sodesawa, T.; Sato, S. Analysis of Heat-Treated Graphite Oxide by X-ray Photoelectron Spectroscopy. *J. Mater. Sci.* **2013**, *48*, 8171–8198. [[CrossRef](#)]
27. Golubev, Y.A.; Rozhkova, N.N.; Kabachkov, E.N.; Shul'ga, Y.M.; Natkaniec-Holderna, K.; Natkaniec, I.; Antonets, I.V.; Makeev, B.A.; Popova, N.A.; Popova, V.A.; et al. Sp² Amorphous Carbons in View of Multianalytical Consideration: Normal, Expected and New. *J. Non-Cryst. Solids* **2019**, *524*, 8171–8198. [[CrossRef](#)]
28. Stankovich, S.; Dikin, D.A.; Piner, R.D.; Kohlhaas, K.A.; Kleinhammes, A.; Jia, Y.; Wu, Y.; Nguyen, S.T.; Ruoff, R.S. Synthesis of Graphene-Based Nanosheets via Chemical Reduction of Exfoliated Graphite Oxide. *Carbon* **2007**, *45*, 1558–1565. [[CrossRef](#)]

29. Stobinski, L.; Lesiak, B.; Malolepszy, A.; Mazurkiewicz, M.; Mierzwa, B.; Zemek, J.; Jiricek, P.; Bieloshapka, I. Graphene Oxide and Reduced Graphene Oxide Studied by the XRD, TEM and Electron Spectroscopy Methods. *J. Electron. Spectrosc. Relat. Phenom.* **2014**, *195*, 145–154. [[CrossRef](#)]
30. Voylov, D.N.; Agapov, A.L.; Sokolov, A.P.; Shulga, Y.M.; Arbuzov, A.A. Room Temperature Reduction of Multilayer Graphene Oxide Film on a Copper Substrate: Penetration and Participation of Copper Phase in Redox Reactions. *Carbon* **2014**, *69*, 563–570. [[CrossRef](#)]
31. Yang, H.; Guo, P.; Wang, R.; Chen, Z.; Xu, H.; Pan, H.; Sun, D.; Fang, F.; Wu, R. Sequential Phase Conversion-Induced Phosphides Heteronanorod Arrays for Superior Hydrogen Evolution Performance to Pt in Wide pH Media. *Adv. Mater.* **2022**, *34*, 2107548. [[CrossRef](#)] [[PubMed](#)]
32. Zhang, B.-W.; Cao, L.; Tang, C.; Tan, C.; Cheng, N.; Lai, W.-H.; Wang, Y.-X.; Cheng, Z.-X.; Dong, J.; Kong, Y.; et al. Atomically Dispersed Dual-Site Cathode with a Record High Sulfur Mass Loading for High-Performance Room-Temperature Sodium–Sulfur Batteries. *Adv. Mater.* **2022**, *34*, 2206828. [[CrossRef](#)] [[PubMed](#)]